This article has been accepted for publication in IEEE Wireless Communications Letters. This is the author's version which has not been fully edited and content may change prior to final publication. Citation information: DOI 10.1109/LWC.2024.3442170

RIS-Assisted Receive Generalized Space Shift Keying and Receive Generalized Spatial Modulation

Porfirio A. Marín, Muhammad Hanif, *Senior Member, IEEE,* and Ebrahim Bedeer, *Member, IEEE*

***Abstract*—In this paper, we enhance the performance of wireless communication systems by utilizing reconfigurable intelligent surface (RIS) and index modulation (IM). In particular, we introduce two schemes: RIS-assisted receive generalized space-shift keying (RIS-RGSSK) and RIS-assisted receive generalized spatial modulation (RIS-RGSM). In the RIS-RGSSK scheme, information bits are conveyed through selection of *multiple receive antennas*. The RIS-RGSM scheme takes RIS-RGSSK a step further by conveying information bits not only through the selection of *multiple receive antennas*, but also through embedding information bits in the phase of the received signals using M-ary phase shift keying (PSK) modulation. We also present simple yet efficient greedy detectors (GDs) for non-coherent detection of both schemes. Simulation results demonstrate the advantages of our proposed methods over existing schemes such as the RIS-assisted receive quadrature space-shift keying (RIS-RQSSK).**

***Index Terms*—Receive generalized space-shift keying (RGSSK), receive generalized spatial modulation (RGSM), RIS.**

I. INTRODUCTION

To meet the growing data rate demands, researchers explore technologies to control the propagation channel, leading to the popularity of reconfigurable intelligent surface (RIS) as a potential approach for future wireless communications [1]. Recently, RIS garnered attention from both academia and industry as a candidate solution to improve the spectrum utilization and energy efficiency (EE) [1], [2], [3]. Another paradigm that is gaining interest in advancing communication systems is index modulation (IM) [4]. With IM schemes, the transmission of information bits occurs by activating or deactivating transmission/reception entities, including transmit antennas, receive antennas, and/or subcarriers, among others. This introduces new dimensions for efficient information conveyance, potentially enhancing spectral efficiency (SE), while deactivating entities results in less power consumption while carrying extra information bits, which improves the EE of IM systems [4].

To obtain the benefits of IM in RIS-assisted systems, the authors in [5] proposed the RIS-assisted space shift keying (RIS-SSK), which makes real-time adjustments to the RIS for maximizing the instantaneous signal-to-noise-ratio (SNR) at *one receive antenna*. Following this, in [6] and [7], the spatial modulation (SM) principle is applied to a RIS-based system to transmit additional information bits utilizing the on-off stated of the RIS. In [8], a RIS-based receive antenna space-shift keying (RIS-RSSK) and a RIS-based receive spatial modulation (RIS-RSM) are introduced. The RIS-RSSK conveys information bits through *a single selected receive antenna* index using IM, while RIS-RSM uses IM selection along with additional bits through ordinary M-ary modulation. However, both schemes can only activate *one receive antenna* per IM symbol. The idea in [8] is extended in [9] with the introduction of the RIS-assisted receive quadrature space-shift keying (RIS-RQSSK), allowing the selection of *two receive antennas* independently in the real and imaginary dimensions. While RIS-RQSSK in [9] can also transmit extra bits, it is limited to transmitting only *one extra information bit per each of the only two antennas that can be selected*. In [10], the RIS-assisted receive quadrature spatial modulation (RIS-RQSM) scheme uses *two activated antenna indices* to convey spatial bits, and it transmits additional bits through ordinary M-ary modulation.

In this paper, inspired by the works in [8], [9], we present a RIS-assisted receive generalized space-shift keying (RIS-RGSSK), which operates based on the principle of generalized space-shift keying (GSSK), wherein *multiple antennas are chosen at the receiver*. Additionally, we present a RIS-assisted receive generalized spatial modulation (RIS-RGSM) scheme, where not only information bits are conveyed through the indexes of selected *multiple receive antennas*, but additional information bits are also conveyed via the received signal phase (i.e., using M-ary phase shift keying (PSK) modulation) at each selected antenna. The proposed RIS-RGSSK system optimizes the phase shift of the RIS reflecting elements to maximize the minimum value of the real part of the received signals at all the selected antennas. We choose the real part of the received signal instead of its squared absolute value (or, equivalently, the SNR) as in [8], [9] because it allows us to embed extra information in the phase of the transmitted signal in the proposed RIS-RGSM scheme. We also present non-coherent greedy detectors (GDs) for both schemes. Simulation results quantify the tradeoff between the SE and error rate performance of the proposed schemes when compared to competing schemes from the literature.

The paper proceeds as follows: Section II details the RIS-RGSSK and RIS-RGSM systems model. In Section III, we formulate and solve optimization problems for both schemes. Section IV includes simulations, and comparisons with a benchmark scheme. Finally, Section V concludes the paper.

II. SYSTEM MODEL

This section presents the system model used in the paper. We utilize the RIS as an access point to convey information through the phases of its N reflecting elements to a receiver equipped with K antennas. The RIS elements reflect the incident waves from a nearby RF source. The phases of the reflected waves are controlled by an RIS controller, which receives information bits as an input as shown in Fig. 1.

Porfirio A. Marín and Ebrahim Bedeer are with the Department of Electrical and Computer Engineering, University of Saskatchewan, Saskatoon, Canada S7N 5A9. Emails: {porfirio.marin, e.bedeer}@usask.ca.

Muhammad Hanif is with the Department of Engineering, Thompson Rivers University, Kamloops, Canada V2C 0C8. E-mail: mhanif@tru.ca.

This article has been accepted for publication in IEEE Wireless Communications Letters. This is the author's version which has not been fully edited and content may change prior to final publication. Citation information: DOI 10.1109/LWC.2024.3442170

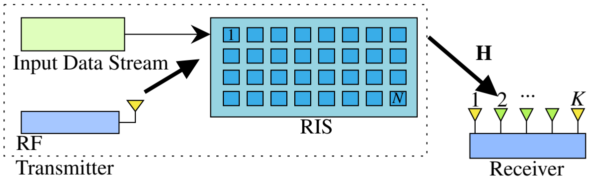

Fig. 1: A schematic of the proposed RIS-RGSSK system.

We denote the baseband complex channel gains between the RIS elements and the kth receive antenna by

$\mathbf{h}_k = \begin{bmatrix} h_{k,1}, & h_{k,2}, & \cdots, & h_{k,N} \end{bmatrix}$, where $k = 1, 2, \cdots, K$. The baseband receive signal at the kth receive antenna is

$$y_k = \sqrt{E_s}\mathbf{h}_k \boldsymbol{\theta} + n_k, \tag{1}$$

where E_s is the energy of the RF waves reflected by each RIS element per IM symbol, n_k denotes the additive white Gaussian noise at the kth receive antenna having zero mean and variance of σ^2, and $\boldsymbol{\theta}$ is the N-dimensional complex vector, whose ith entry, θ_i, represents the reflection coefficient of the ith reflecting element for $i = 1, 2, \cdots, N$. In this work, we assume lossless reflection from the RIS elements, i.e., $|\theta_i| = 1$ for $i = 1, 2, \cdots, N$.

In the proposed RIS-RGSSK scheme, a total of L receive antennas are selected to convey the information bits. Since there are a total of $\binom{K}{L}$ combinations of L receive antennas, the RIS-RGSSK utilizes $\lfloor \log_2 \binom{K}{L} \rfloor$ information bits of a transmit symbol to select a combination of the receive antennas. Subsequently, we extend the RIS-RGSSK to the RIS-RGSM, where we use M-ary PSK symbols to convey the additional information bits. Therefore, for the RIS-RGSM, the total number of bits per each transmit IM symbol is given by $\mathcal{B} = \lfloor \log_2 \binom{K}{L} \rfloor + L \log_2(M)$. We denote the ordered set of selected receive-antenna indexes by $\mathcal{S}$ and its lth element by $\mathcal{S}(l)$ for $l = 1, \cdots, L$. Without loss of generality, we assume that $\mathcal{S}(1) < \mathcal{S}(2) < \cdots < \mathcal{S}(L)$, and we denote $\mathcal{C}$ as the codewords set, i.e., the set of all combinations of receive-antenna indexes used at the transmitter. The real part of the signal received at the lth selected antenna is given by

$$y^{\mathcal{R}}_{\mathcal{S}(l)} = \sqrt{E_s}\left(\mathbf{h}^{\mathcal{R}}_{\mathcal{S}(l)}\boldsymbol{\theta}^{\mathcal{R}} - \mathbf{h}^{\mathcal{I}}_{\mathcal{S}(l)}\boldsymbol{\theta}^{\mathcal{I}}\right) + n^{\mathcal{R}}_{\mathcal{S}(l)}. \tag{2}$$

Here, $(\cdot)^{\mathcal{R}}$ and $(\cdot)^{\mathcal{I}}$ denote the real and imaginary part, respectively, of a complex scalar/vector.

In the following, we initially present the optimization problem for the proposed RIS-RGSSK scheme. For which, we select the real part of the received signal as our objective function, which means that we use only the in-phase channel for further processing. Its solution is obtained by solving the KKT conditions. Then, we extend the solution to the RIS-RGSM scheme in Section III-B. We also present non-coherent GDs for both schemes, which have significantly reduced computational complexity than the optimal maximum-likelihood (ML) detectors.

III. Problem Formulation and Solution

A. RIS-RGSSK Scheme

In this scheme, we maximize the minimum of the transmitted signal components in the real part of the received signals at all the selected antennas. Here, unlike [9], we have not used both real and imaginary components of the received signal in the objective function. This change enables us 1) to select more than two receive antennas, which is not possible in the schemes presented in [9] and 2) to obtain a low-complexity optimal solution that can be applied to the RIS-RGSM.

The RIS-RGSSK optimization problem is formulated as

$$\mathcal{P}1: \max_{\boldsymbol{\theta}^{\mathcal{R}}, \boldsymbol{\theta}^{\mathcal{I}}} \min_{l \in \{1,2,\cdots,L\}} \{\mathbf{h}^{\mathcal{R}}_{\mathcal{S}(l)}\boldsymbol{\theta}^{\mathcal{R}} - \mathbf{h}^{\mathcal{I}}_{\mathcal{S}(l)}\boldsymbol{\theta}^{\mathcal{I}}\}, \tag{3}$$

$$\text{s.t.}\ \left(\theta_i^{\mathcal{R}}\right)^2 + \left(\theta_i^{\mathcal{I}}\right)^2 = 1, \quad \forall\, i = 1, 2, \cdots, N. \tag{4}$$

The problem $\mathcal{P}1$ is re-expressed using the epigraph form as

$$\mathcal{P}2: \min_{\boldsymbol{\theta}^{\mathcal{R}}, \boldsymbol{\theta}^{\mathcal{I}}, t} f_0(\boldsymbol{\theta}^{\mathcal{R}}, \boldsymbol{\theta}^{\mathcal{I}}, t) \triangleq t \tag{5}$$

$$\text{s.t.}\ f_l(\boldsymbol{\theta}^{\mathcal{R}}, \boldsymbol{\theta}^{\mathcal{I}}, t) \triangleq -\mathbf{h}^{\mathcal{R}}_{\mathcal{S}(l)}\boldsymbol{\theta}^{\mathcal{R}} + \mathbf{h}^{\mathcal{I}}_{\mathcal{S}(l)}\boldsymbol{\theta}^{\mathcal{I}} - t \leq 0, \tag{6}$$

$$g_i(\boldsymbol{\theta}^{\mathcal{R}}, \boldsymbol{\theta}^{\mathcal{I}}, t) \triangleq \left(\theta_i^{\mathcal{R}}\right)^2 + \left(\theta_i^{\mathcal{I}}\right)^2 - 1 = 0, \tag{7}$$

for $l = 1, \cdots, L$, and $i = 1, 2, \cdots, N$. Note that the problem $\mathcal{P}2$ is non-convex due to the equality constraints in (7). The Lagrange function associated with the problem $\mathcal{P}2$ is given by

$$G(\boldsymbol{\theta}^{\mathcal{R}}, \boldsymbol{\theta}^{\mathcal{I}}, t, \boldsymbol{\lambda}, \boldsymbol{\nu}) = t + \sum_{l=1}^{L} \lambda_l f_l(\boldsymbol{\theta}^{\mathcal{R}}, \boldsymbol{\theta}^{\mathcal{I}}, t) + \sum_{i=1}^{N} \nu_i g_i(\boldsymbol{\theta}^{\mathcal{R}}, \boldsymbol{\theta}^{\mathcal{I}}, t), \tag{8}$$

where $\boldsymbol{\lambda} = \begin{bmatrix}\lambda_1, \cdots, \lambda_L\end{bmatrix}^T \geq 0$ and $\boldsymbol{\nu} = \begin{bmatrix}\nu_1, \nu_2, \cdots, \nu_N\end{bmatrix}^T$ are the Lagrange multiplier vectors corresponding to the inequality and equality constraints. Using (6) and (7), we get

$$\begin{aligned} G(\boldsymbol{\theta}^{\mathcal{R}}, \boldsymbol{\theta}^{\mathcal{I}}, t, \boldsymbol{\lambda}, \boldsymbol{\nu}) = &\left(1 - \sum_{l=1}^{L} \lambda_l\right) t \\ &+ \sum_{l=1}^{L} \lambda_l \left(-\mathbf{h}^{\mathcal{R}}_{\mathcal{S}(l)}\boldsymbol{\theta}^{\mathcal{R}} + \mathbf{h}^{\mathcal{I}}_{\mathcal{S}(l)}\boldsymbol{\theta}^{\mathcal{I}}\right) \\ &+ \sum_{i=1}^{N} \nu_i \left(\left(\theta_i^{\mathcal{R}}\right)^2 + \left(\theta_i^{\mathcal{I}}\right)^2 - 1\right). \end{aligned} \tag{9}$$

The objective function of the dual optimization problem can be obtained from (9) as

$$q(\boldsymbol{\lambda}, \boldsymbol{\nu}) = \inf_{\boldsymbol{\theta}^{\mathcal{R}}, \boldsymbol{\theta}^{\mathcal{I}}, t} G(\boldsymbol{\theta}^{\mathcal{R}}, \boldsymbol{\theta}^{\mathcal{I}}, t, \boldsymbol{\lambda}, \boldsymbol{\nu}). \tag{10}$$

By setting the gradients of $G(\boldsymbol{\theta}^{\mathcal{R}}, \boldsymbol{\theta}^{\mathcal{I}}, t, \boldsymbol{\lambda}, \boldsymbol{\nu})$ with respect to $\boldsymbol{\theta}^{\mathcal{R}}$, $\boldsymbol{\theta}^{\mathcal{I}}$, and t to zero, we obtain the optimal θ_i's as

$$\tilde{\theta}_i = \frac{\sum_{l=1}^{L} \lambda_l h^*_{\mathcal{S}(l),i}}{2\nu_i}, \quad i = 1, ..., N, \tag{11}$$

where $(\cdot)^*$ denotes the conjugation operation and $\sum_{l=1}^{L} \lambda_l = 1$. Note that the Lagrange function in (9) is quadratic in $\boldsymbol{\theta}^{\mathcal{R}}$ and $\boldsymbol{\theta}^{\mathcal{I}}$. Therefore, the $q(\boldsymbol{\lambda}, \boldsymbol{\nu})$ would be finite only if $\boldsymbol{\nu} > 0$.

Using (11) and $\sum_{l=1}^{L}\lambda_l=1$, $\mathcal{P}2$ can be expressed as

$$\mathcal{P}3:\min_{\boldsymbol{\lambda},\boldsymbol{\nu}} -q(\boldsymbol{\lambda},\boldsymbol{\nu}) \tag{12}$$

$$\text{s.t.} \sum_{l=1}^{L}\lambda_l=1, \tag{13}$$

$$\lambda_l\geq 0,\quad \forall\, l=1,\cdots,L, \tag{14}$$

$$\nu_i>0,\quad \forall\, i=1,2,\cdots,N, \tag{15}$$

where

$$q(\boldsymbol{\lambda},\boldsymbol{\nu})=-\sum_{i=1}^{N}\left(\frac{1}{4\nu_i}\left|\sum_{l=1}^{L}\lambda_l h_{\mathcal{S}(l),i}\right|^2+\nu_i\right). \tag{16}$$

By equating the gradient of $q(\boldsymbol{\lambda},\boldsymbol{\nu})$ with respect to $\boldsymbol{\nu}$ to zero and using the positive solution, we get

$$\tilde{\nu}_i=\frac{1}{2}\left|\sum_{l=1}^{L}\lambda_l h_{\mathcal{S}(l),i}\right|. \tag{17}$$

By using (17), the problem $\mathcal{P}3$ simplifies to

$$\mathcal{P}4:\min_{\boldsymbol{\lambda}}\sum_{i=1}^{N}\left|\sum_{l=1}^{L}\lambda_l h_{\mathcal{S}(l),i}\right| \tag{18}$$
$$\text{s.t. (13) and (14).}$$

The equality constraint in the above optimization problem can be removed by substituting $\lambda_L=1-\sum_{l=1}^{L-1}\lambda_l$ in the objective function. The updated optimization problem becomes

$$\mathcal{P}5:\min_{\boldsymbol{\lambda}}\sum_{i=1}^{N}\left|h_{\mathcal{S}(L),i}+\sum_{l=1}^{L-1}\lambda_l\left(h_{\mathcal{S}(l),i}-h_{\mathcal{S}(L),i}\right)\right| \tag{19}$$

$$\text{s.t.}\sum_{l=1}^{L-1}\lambda_l\leq 1, \tag{20}$$

$$\lambda_l\geq 0,\quad \forall\, l=1,\cdots,L-1. \tag{21}$$

For this problem $\mathcal{P}5$, the associated Lagrange function is

$$G^{(1)}\left(\boldsymbol{\lambda},\boldsymbol{\alpha},\beta\right)=\sum_{i=1}^{N}\left|A_i(\boldsymbol{\lambda})\right|-\sum_{l=1}^{L-1}\alpha_l\lambda_l+\beta\left(\sum_{l=1}^{L-1}\lambda_l-1\right), \tag{22}$$

where $\beta\geq 0$ and $\alpha_l\geq 0$ are the Lagrange multipliers, and

$$A_i(\boldsymbol{\lambda})=h_{S(L),i}+\sum_{j=1}^{L-1}\lambda_j\left(h_{S(j),i}-h_{S(L),i}\right). \tag{23}$$

Since $\mathcal{P}5$ is a convex problem, any points satisfying the KKT conditions are primal and dual optimal. Thus, for the problem (22), the KKT conditions, $\forall\, l=1,\cdots,L-1$, are stated as: $\tilde{\lambda}_l\geq 0$, $\sum_{l=1}^{L-1}\tilde{\lambda}_l-1\leq 0$, $\tilde{\alpha}_l\geq 0$, $\tilde{\beta}\geq 0$, $\tilde{\alpha}_l\tilde{\lambda}_l=0$,

$$\tilde{\beta}\left(\sum_{l=1}^{L-1}\tilde{\lambda}_l-1\right)=0, \tag{24}$$

$$\sum_{i=1}^{N}\frac{\left(\left(h_{S(l),i}-h_{S(L),i}\right)^{*}A_i(\tilde{\boldsymbol{\lambda}})\right)^{\mathcal{R}}}{\left|A_i(\tilde{\boldsymbol{\lambda}})\right|}-\tilde{\alpha}_l+\tilde{\beta}=0. \tag{25}$$

From the KKT conditions, we have a total of 2^L cases corresponding to whether $\tilde{\lambda}_l=0$ or $\tilde{\lambda}_l>0$ for $l=1,\cdots,L-1$ and $1-\sum_{j=1}^{L-1}\tilde{\lambda}_j=\tilde{\lambda}_L=0$, or $\tilde{\lambda}_L>0$. Among all the cases, $\tilde{\lambda}_l=0$ for $l=1,2,\cdots,L$ is infeasible, as $\tilde{\lambda}_L=1-\sum_{j=1}^{L-1}\tilde{\lambda}_j$. As such, at least one of $\tilde{\lambda}_l$'s, $l=1,2,\cdots,L$, must be positive. Without loss of generality, we assume that, $\tilde{\lambda}_L=1-\sum_{j=1}^{L-1}\tilde{\lambda}_j>0$. Consequently, (24) implies that $\tilde{\beta}=0$. Therefore, (25) simplifies to

$$f\left(\tilde{\boldsymbol{\lambda}},l\right)\triangleq\sum_{i=1}^{N}\frac{\left(\left(h_{S(l),i}-h_{S(L),i}\right)^{*}A_i(\tilde{\boldsymbol{\lambda}})\right)^{\mathcal{R}}}{\left|A_i(\tilde{\boldsymbol{\lambda}})\right|}=\tilde{\alpha}_l. \tag{26}$$

From the KKT conditions, we can have the following two cases for each l: $\tilde{\alpha}_l>0$ and $\tilde{\lambda}_l=0$; and $\tilde{\alpha}_l=0$. For the first case, $A_i(\boldsymbol{\lambda})$, as defined in (23), becomes independent of $h_{\mathcal{S}(l),i}$ because of $\tilde{\lambda}_l=0$. Using the central-limit theorem, it can be shown that it is extremely unlikely that $f(\boldsymbol{\lambda},l)$, as defined in (26), becomes positive. As such, the first case is extremely unlikely to occur. In other words, the second case, i.e., $\tilde{\alpha}_l=0$, will occur with very high probability, and (25) simplifies to

$$f\left(\tilde{\boldsymbol{\lambda}},l\right)=\sum_{i=1}^{N}\frac{\left(\left(h_{S(l),i}-h_{S(L),i}\right)^{*}A_i(\tilde{\boldsymbol{\lambda}})\right)^{\mathcal{R}}}{\left|A_i(\tilde{\boldsymbol{\lambda}})\right|}=0, \tag{27}$$

for $l=1,\cdots,L-1$. Consequently, solving the optimization problem (3) reduces to solving a system of L equations formed by $\sum_{l=1}^{L}\lambda_l=1$ and (27), then $\{\tilde{\nu}_i\}$ is obtained via (17), and the reflection coefficients $\left\{\tilde{\theta}_i\right\}$ are obtained by substituting (17) in (11), which is expressed as follows

$$\tilde{\theta}_i=\frac{\sum_{l=1}^{L}\tilde{\lambda}_l h^{*}_{\mathcal{S}(l),i}}{\left|\sum_{l=1}^{L}\tilde{\lambda}_l h_{\mathcal{S}(l),i}\right|},\forall\, i=1,2,\cdots,N. \tag{28}$$

RIS-RGSSK Reception: The ML detector of the RIS-RGSSK scheme is given by

$$\hat{\mathcal{S}}_{\mathrm{ML}}=\arg\min_{\mathcal{S}}\sum_{k=1}^{K}\left|y_k-\sqrt{E_s}\mathbf{h}_k\widetilde{\boldsymbol{\theta}}\left(\mathcal{S}\right)\right|^2, \tag{29}$$

where $\widetilde{\boldsymbol{\theta}}\left(\mathcal{S}\right)$ is the vector of optimal phase shifts of the RIS elements corresponding to the selected antennas $\mathcal{S}$ as given by (28). Observe that the ML receiver requires the complete channel state information (CSI) at the receiver. Moreover, it is computationally intensive. To address these issues with the optimal ML receiver, we present the following low-complexity GD.

The proposed GD determines the selected receive antennas without requiring CSI. First, the detector estimates $L-1$ indexes as $\hat{\mathcal{S}}_1=\arg\max_{\text{L-1}1\leq l\leq K}\left\{y_l^{\mathcal{R}}\right\}$, where $\arg\max_{\text{L-1}}\{\cdot\}$ returns the set of $L-1$ maximum values. The estimated set $\hat{\mathcal{S}}_1$ is then used to find the range of the last index using the final-index range finder proposed in [11]. We denote the range of the last index by r, which guarantees that the estimated index set, $\hat{\mathcal{S}}$, lies in the code book used at the transmitter, $\mathcal{C}$. Then, the last index is estimated as $\hat{l}_F=\arg\max_{l\in r}\left\{y_l^{\mathcal{R}}\right\}$. Finally, $\hat{\mathcal{S}}$ is obtained by sorting the elements of $\hat{\mathcal{S}}_1\cup\{\hat{l}_F\}$.

B. RIS-RGSM Scheme

In the following, we first explain the proposed RIS-RGSM scheme for single receive antenna selection, and then we extend it to the selection of more than one receive antenna. For single receive antenna selection (i.e., when $L = 1$), the proposed RIS-RGSSK scheme optimizes $\boldsymbol{\theta}$ as $\tilde{\theta}_i = h^*_{\mathcal{S}(1),i}/|h_{\mathcal{S}(1),i}|$, for $i = 1, 2, \cdots, N$ as $\sum_{l=1}^{L} \lambda_l = 1$ simplifies to $\lambda_1 = 1$. In order to convey additional information using a PSK-modulated symbol, we modify $\tilde{\theta}_i$ as

$$\tilde{\theta}_i = x_1 \frac{h^*_{\mathcal{S}(1),i}}{|h_{\mathcal{S}(1),i}|} = \frac{\left(x_1^* h_{\mathcal{S}(1),i}\right)^*}{|x_1^* h_{\mathcal{S}(1),i}|}, \tag{30}$$

where x_1 is the PSK-modulated symbol with unit power, i.e., $|x_1| = 1$. The modification, as given by (30), ensures that the received signal at the selected antenna depends on the phase of the PSK-modulated symbol x_1. From (30), $\boldsymbol{\theta}$ can also be obtained by solving the following optimization problem

$$\tilde{\boldsymbol{\theta}} = \underset{\left(\theta_i^{\mathcal{R}}\right)^2 + \left(\theta_i^{\mathcal{I}}\right)^2 = 1}{\arg\max} \left(x_1^* \mathbf{h}_{\mathcal{S}(1)}\right)^{\mathcal{R}} \boldsymbol{\theta}^{\mathcal{R}} - \left(x_1^* \mathbf{h}_{\mathcal{S}(1)}\right)^{\mathcal{I}} \boldsymbol{\theta}^{\mathcal{I}}. \tag{31}$$

Note that if the absolute value had been used instead of the real part of $x_1^* \mathbf{h}_{\mathcal{S}(1)} \boldsymbol{\theta}$, the solution would not have been unique. As a result, the objective function maximizing the objective function would not ensure that the received signal at the selected receive antenna depends on the phase of the PSK-modulated symbol x_1. That explains why we choose the real part instead of the absolute value of the transmitted signal component as the objective function in the optimization problems for both RIS-RGSSK and RIS-RGSM schemes.

For the selection of more than one receive antenna, the proposed RIS-RGSM scheme generalizes the optimization problem given in (31) as follows

$$\mathcal{P}6 : \max_{\boldsymbol{\theta}^{\mathcal{R}}, \boldsymbol{\theta}^{\mathcal{R}}} \min_{l \in \{1,2,\cdots,L\}} \left\{ \left(x_l^* \mathbf{h}_{\mathcal{S}(l)}\right)^{\mathcal{R}} \boldsymbol{\theta}^{\mathcal{R}} - \left(x_l^* \mathbf{h}_{\mathcal{S}(l)}\right)^{\mathcal{I}} \boldsymbol{\theta}^{\mathcal{I}} \right\}, \tag{32}$$

$$\text{s.t. } \left(\theta_i^{\mathcal{R}}\right)^2 + \left(\theta_i^{\mathcal{I}}\right)^2 = 1, \quad \forall\, i = 1, 2, \cdots, N. \tag{33}$$

The problem $\mathcal{P}6$ is closely related to the problem $\mathcal{P}1$, with the only difference that $\mathbf{h}_{\mathcal{S}(l)}$ is replaced by $x_l^* \mathbf{h}_{\mathcal{S}(l)}$. Hence, similar to the proposed RIS-RGSSK scheme, $\tilde{\boldsymbol{\theta}}$ for the proposed RIS-RGSM scheme is obtained as

$$\tilde{\theta}_i = \frac{\sum_{l=1}^{L} \tilde{\lambda}_l x_l h^*_{\mathcal{S}(l),i}}{\left|\sum_{l=1}^{L} \tilde{\lambda}_l x_l^* h_{\mathcal{S}(l),i}\right|}, \quad \forall\, i = 1, 2, \cdots, N, \tag{34}$$

where $\tilde{\lambda}_l$ for $l = 1, 2, \cdots, L$ are obtained using $\tilde{\lambda}_L = 1 - \sum_{j=1}^{L-1} \tilde{\lambda}_j$, and solving the following $L-1$ equations simultaneously.

$$\sum_{i=1}^{N} \frac{\left(\left(x_l^* h_{S(l),i} - x_L^* h_{S(L),i}\right)^* B_i(\tilde{\boldsymbol{\lambda}})\right)^{\mathcal{R}}}{\left|B_i(\tilde{\boldsymbol{\lambda}})\right|} = 0, \tag{35}$$

for

$$B_i(\tilde{\boldsymbol{\lambda}}) = x_L^* h_{S(L),i} + \sum_{j=1}^{L-1} \tilde{\lambda}_j \left(x_j^* h_{S(j),i} - x_L^* h_{S(L),i}\right). \tag{36}$$

RIS-RGSM Reception: Similar to the RIS-RGSSK scheme, the optimal ML detector can be shown to be

$$\left(\hat{\mathcal{S}}_{\mathrm{ML}}, \hat{x}_{\mathrm{ML}}\right) = \arg\min_{\mathcal{S},x} \sum_{k=1}^{K} \left| y_k - \sqrt{E_s}\mathbf{h}_k \widetilde{\boldsymbol{\theta}}\left(\mathcal{S}, x\right)\right|^2, \tag{37}$$

where $\widetilde{\boldsymbol{\theta}}\left(\mathcal{S}, x\right)$ is the vector of optimum phase shifts of the RIS elements corresponding to both the selected antennas $\mathcal{S}$ and the extra information bits x. Since the optimal receiver requires the complete CSI and is highly computationally intensive, we present the following GD.

For the proposed GD, the receiver first detects the selected receive antenna indexes without requiring any CSI and then retrieves the extra information bits $\hat{x}_l$ from the phase of the received signal at estimated receive antenna indexes. Similar to the RIS-RGSSK scheme, the RIS-RGSM receiver estimates the receive antenna indexes by first finding the $L-1$ indexes $\hat{\mathcal{S}}_1 = \arg\max_{\mathrm{L\text{-}1} 1 \le l \le K} |y_l|$ and then estimating the last index $\hat{l}_F = \arg\max_{l \in r} |y_l|$. The estimated set $\hat{\mathcal{S}}$ is obtained by sorting the elements of $\hat{\mathcal{S}}_1 \cup \{\hat{l}_F\}$. After estimating the selected indexes, the transmitted M-PSK symbols are estimated non-coherently as

$$\hat{x}_l = \underset{x_l \in \mathcal{X}}{\arg\max} \left\{ \left(y_{\hat{\mathcal{S}}(l)} x_l^*\right)^{\mathcal{R}} \right\}, \quad \forall\, l = 1, \cdots, L, \tag{38}$$

where $\arg\max\{\cdot\}$ returns the maximum value of its argument, and $\mathcal{X}$ is the M-PSK modulating set used at the transmitter.

C. Complexity Analysis

In the following, we provide the computational complexities of the proposed greedy and the optimal ML detectors.

For the RIS-RGSM, the computational complexity of the proposed GD is as follows: The detection of the L maximum values out of K values of the real part of the received signal has a complexity of $O(K \log L)$. Also, retrieving the extra information bits through (38) is of $O(LM)$. As such, the complexity of the GD for RIS-RGSM scheme is given by $O(K \log L + LM)$. For the RIS-RGSSK scheme, the computational complexity is just $O(K \log L)$.

For the optimal ML detector in (37), the optimal phase calculation as given by (34) requires solving a set of L equations to determine optimal λ's, whose complexity is $O(L^3)$. Given optimal λ's, the complexity of (34) is $O(NL)$. Since the optimal phase values are computed $M\binom{K}{L}$ times, the complexity of the optimal phase calculation is $O\left(M(L^3 + NL)K^L\right)$. Furthermore, (37) requires evaluation of K dot products of vectors of size N for each of $M\binom{K}{L}$ combinations. As such, the complexity of implementing (37) given the optimal phase values is $O\left(NMK^{L+1}\right)$. Using the afore-mentioned complexities, the computational complexity of the optimal ML detector can be shown to be $O\left(M(L^3 + KN) \cdot K^L\right)$. For the RIS-RGSKK scheme, the complexity can similarly be shown to be $O\left((L^3 + KN) \cdot K^L\right)$.

Observe that the proposed GDs have significantly less computational complexity than the ML detectors.

IV. Simulation Results

In this section, we present simulation results to evaluate the performance of the proposed RIS-RGSSK and RIS-RGSM

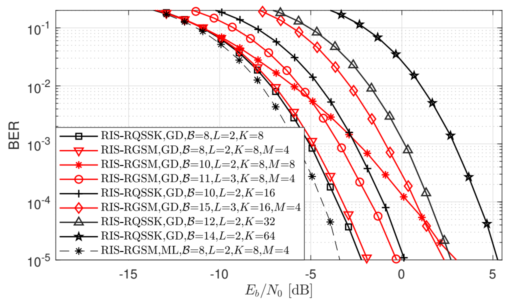

Fig. 2: Comparison of the proposed RIS-RGSM (with $K = 8$, and 16) and the RIS-RQSSK (with $K = 8$, 16, 32, and 64) schemes for $L = 2$, and 3, at $N = 128$.

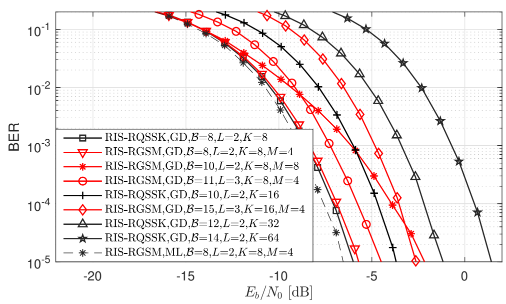

Fig. 3: Comparison of the proposed RIS-RGSM (with $K = 8$, and 16) and the RIS-RQSSK (with $K = 8$, 16, 32, and 64) schemes for $L = 2$, and 3, at $N = 256$.

schemes. Here, we define the SNR in dB to be equal to E_s/N_0, and the relation between E_s/N_0 and E_b/N_0 is given as $E_b/N_0 = E_s/N_0 + 10\log_{10}(N \times K) - 10\log_{10}(\mathcal{B})$. Following [9], a key point to observe is the consistent relationship between the elements of optimal $\tilde{\boldsymbol{\lambda}}$. Taking into consideration that all $h^{\mathcal{R}}_{S(l),i}$, $h^{\mathcal{I}}_{S(l),i}$, $l = 1, ..., L$ and $i = 1, 2, ..., N$, are RVs identically distributed as $\mathcal{N}\left(0, \frac{1}{2}\right)$, this implies that $\tilde{\lambda}_l$, $\forall\ l = 1, \cdots, L$, as calculated from (27) or (35) have equal mean, i.e., $\mathbb{E}\{\tilde{\lambda}_l\} = 1/L$, $l = 1, ..., L$.

Fig. 2 illustrates the BER of our proposed RIS-RGSM scheme compared to the RIS-RQSSK scheme (with polarity bits) from [9], with $N = 128$. Various configurations are presented for the RIS-RGSM scheme to achieve $\mathcal{B} = 8$, 10, 11, and 15. For the RIS-RQSSK with $K = 8$, 6 bits are conveyed through index selection, and an additional 1 bit is transmitted per selected antenna, resulting in a total $\mathcal{B} = 6+2 = 8$ bits per symbol. In the case where both schemes operate with $\mathcal{B} = 8$, the proposed RIS-RGSM demonstrates competitive performance, trailing RIS-RQSSK by only 0.3 dB at a BER of 10^{-5}. Furthermore, increasing M beyond 4, e.g., using 8-PSK while selecting $L = 2$ out of $K = 8$ antennas, results in a degradation of BER performance at higher E_b/N_0. Upon increasing $\mathcal{B}$ to 11 for the RIS-RGSM scheme ($L = 3$ out of $K = 8$ using QPSK) and the RIS-RQSSK achieving $\mathcal{B} = 10$ (with $K = 16$ and $L = 2$), our proposed RIS-RGSM outperforms the RIS-RQSSK by 0.6 dB, transmitting 10% more bits. Additionally, at $\mathcal{B} = 15$ ($L = 3$ out of $K = 16$ using QPSK), the proposed RIS-RGSM exhibits a noteworthy 3.0 dB improvement in BER compared to the RIS-RQSSK at $\mathcal{B} = 14$ ($K = 64$ and $L = 2$).

In Fig. 3, we depict the BER performance for the parameters used in Fig. 2 but for $N = 256$. The results show that when $\mathcal{B} = 8$, the BER performance advantage of the RIS-RQSSK becomes less significant compared to our RIS-RGSM as N increases from 128 to 256, presenting a margin of only 0.2 dB for the same BER of 10^{-5}. Overall, the results show that for higher $\mathcal{B}$ and larger N, our proposed RIS-RGSM can evidently outperforms the RIS-RQSSK, e.g., 4.0 dB improvement in E_b/N_0 of the proposed RIS-RGSM ($\mathcal{B} = 15$) compared to the RIS-RQSSK ($\mathcal{B} = 14$). One can also see from Fig. 2 and Fig. 3 that the proposed non-coherent GD approaches the ML performance for the same system parameters.

V. Conclusion

In this paper, we explored two innovative schemes, RIS-RGSSK and RIS-RGSM. We introduced these schemes, allowing the selection of multiple receive antennas instead of being limited to one or two. We formulated and solved an optimization problem for RIS-RGSSK, maximizing the real component of the received signal. The proposed RIS-RGSM scheme extends the RIS-RGSSK scheme by embedding extra information in the phase of the transmitted signal using M-PSK modulation by solving an extended optimization problem. Our simulation results showed that, as the number of the RIS reflecting elements increases, the proposed RIS-RGSM can achieve both a better BER performance and a higher bit rate compared to the recent RIS-RQSSK benchmark, e.g., 4.0 dB improvement in E_b/N_0 when N = 256.

References

[1] E. Basar, M. Di Renzo, J. De Rosny, M. Debbah, M.-S. Alouini, and R. Zhang, "Wireless communications through reconfigurable intelligent surfaces," *IEEE Access*, vol. 7, pp. 116 753–116 773, 2019.

[2] X. Zhu, W. Chen, Q. Wu, Z. Li, J. Li, S. Zhang, and M. Ding, "Reconfigurable intelligent surface aided space shift keying with imperfect CSI," *IEEE Internet Things J.*, Nov. 2023.

[3] X. Zhu, L. Yuan, Q. Li, L. Jin, X. Nie, C. Pan, and J. Zhang, "RIS-assisted full-duplex space shift keying: System scheme and performance analysis," *IEEE Trans. Green Commun. Netw.*, Jul. 2023.

[4] J. Li, S. Dang, M. Wen, Q. Li, Y. Chen, Y. Huang, and W. Shang, "Index modulation multiple access for 6G communications: Principles, applications, and challenges," *IEEE Netw.*, vol. 37, no. 1, pp. 52–60, Jan./Feb. 2023.

[5] A. E. Canbilen, E. Basar, and S. S. Ikki, "Reconfigurable intelligent surface-assisted space shift keying," *IEEE Wireless Commun. Lett.*, vol. 9, no. 9, pp. 1495–1499, Jan. 2020.

[6] W. Yan, X. Yuan, Z.-Q. He, and X. Kuai, "Passive beamforming and information transfer design for reconfigurable intelligent surfaces aided multiuser MIMO systems," *IEEE J. Sel. Areas Commun.*, vol. 38, no. 8, pp. 1793–1808, Aug. 2020.

[7] S. Lin, B. Zheng, G. C. Alexandropoulos, M. Wen, M. Di Renzo, and F. Chen, "Reconfigurable intelligent surfaces with reflection pattern modulation: Beamforming design and performance analysis," *IEEE Trans. Wireless Commun.*, vol. 20, no. 2, pp. 741–754, Feb. 2021.

[8] E. Basar, "Reconfigurable intelligent surface-based index modulation: A new beyond MIMO paradigm for 6G," *IEEE Trans. Commun.*, vol. 68, no. 5, pp. 3187–3196, May 2020.

[9] M. H. Dinan, N. S. Perović, and M. F. Flanagan, "RIS-assisted receive quadrature space-shift keying: A new paradigm and performance analysis," *IEEE Trans. Commun.*, vol. 70, no. 3, pp. 6874–6889, Oct. 2022.

[10] M. H. Dinan, M. Di Renzo, and M. F. Flanagan, "RIS-assisted receive quadrature spatial modulation with low-complexity greedy detection," *IEEE Trans. Commun.*, vol. 71, no. 11, pp. 6541–6560, Nov. 2023.

[11] M. Hanif and H. H. Nguyen, "Frequency-shift chirp spread spectrum communications with index modulation," *IEEE Internet Things J.*, vol. 8, no. 24, pp. 17 611–17 621, Dec. 2021.